

# Effects of Ammonium on Intracellular pH in Rat Medullary Thick Ascending Limb: Mechanisms of Apical Membrane $\text{NH}_4^+$ Transport

BRUNS A. WATTS, III and DAVID W. GOOD

From the Departments of Internal Medicine and Physiology and Biophysics, University of Texas Medical Branch, Galveston, Texas 77555-0562

**ABSTRACT** The renal medullary thick ascending limb (MTAL) actively reabsorbs ammonium ions. To examine the effects of  $\text{NH}_4^+$  transport on intracellular pH ( $\text{pH}_i$ ) and the mechanisms of apical membrane  $\text{NH}_4^+$  transport, MTALs from rats were isolated and perfused in vitro with 25 mM  $\text{HCO}_3^-$ -buffered solutions (pH 7.4).  $\text{pH}_i$  was monitored using the fluorescent dye BCECF. In the absence of  $\text{NH}_4^+$ , the mean  $\text{pH}_i$  was 7.16. Luminal addition of 20 mM  $\text{NH}_4^+$  caused a rapid intracellular acidification ( $\text{dpH}_i/\text{dt} = 11.1 \text{ U/min}$ ) and reduced the steady state  $\text{pH}_i$  to 6.67 ( $\Delta\text{pH}_i = 0.5 \text{ U}$ ), indicating that apical  $\text{NH}_4^+$  entry was more rapid than entry of  $\text{NH}_3$ . Luminal furosemide ( $10^{-4} \text{ M}$ ) reduced the initial rate of cell acidification by 70% and the fall in steady state  $\text{pH}_i$  by 35%. The residual acidification observed with furosemide was inhibited by luminal barium (12 mM), indicating that apical  $\text{NH}_4^+$  entry occurred via both furosemide ( $\text{Na}^+\text{-NH}_4^+\text{-2Cl}^-$  cotransport) and barium-sensitive pathways. The role of these pathways in  $\text{NH}_4^+$  absorption was assessed under symmetric ammonium conditions. With 4 mM  $\text{NH}_4^+$  in perfusate and bath, mean steady state  $\text{pH}_i$  was 6.61 and net ammonium absorption was 12 pmol/min/mm. Addition of furosemide to the lumen abolished net ammonium absorption and caused  $\text{pH}_i$  to increase abruptly ( $\text{dpH}_i/\text{dt} = 0.8 \text{ U/min}$ ) to 7.0. Increasing luminal  $[\text{K}^+]$  from 4 to 25 mM caused a similar, rapid cell alkalinization. The pronounced cell alkalinization observed with furosemide or increasing  $[\text{K}^+]$  was not observed in the absence of  $\text{NH}_4^+$ . In symmetric 4 mM  $\text{NH}_4^+$  solutions, addition of barium to the lumen caused a slow intracellular alkalinization and reduced net ammonium absorption only by 14%. Conclusions: (a) ammonium transport is a critical determinant of  $\text{pH}_i$  in the MTAL, with  $\text{NH}_4^+$  absorption markedly acidifying the cells and maneuvers that inhibit apical  $\text{NH}_4^+$  uptake (furosemide or elevation of luminal  $[\text{K}^+]$ ) causing intracellular alkalinization; (b) most or all of transcellular ammonium absorption is mediated by apical membrane  $\text{Na}^+\text{-NH}_4^+\text{-2Cl}^-$  cotransport; (c)  $\text{NH}_4^+$  also permeates a barium-sensitive apical membrane transport pathway (presumably apical membrane  $\text{K}^+$  channels) but this pathway does not contribute significantly to ammonium absorption under physiologic (symmetric ammonium) conditions.

Address correspondence to David W. Good, PhD, Division of Nephrology, 4.200 John Sealy Hospital E62, University of Texas Medical Branch, Galveston, Texas 77555-0562.

## INTRODUCTION

The thick ascending limb of the loop of Henle influences urinary net acid excretion through a unique capacity to reabsorb both ammonium<sup>1</sup> and bicarbonate (Good, Knepper, and Burg, 1984; Knepper, Packer and Good, 1989; Good, 1991, 1993). Studies using isolated, perfused medullary thick ascending limbs (MTAL) have demonstrated that the majority of the ammonium absorption occurs by the active transport of  $\text{NH}_4^+$  (Good, 1988; Garvin, Burg, and Knepper, 1988). The active  $\text{NH}_4^+$  absorption secondarily lowers the luminal  $\text{NH}_3$  concentration to half its value in the peritubular bath (Good et al., 1984; Knepper et al., 1989). Thus, the net ammonium flux occurs in a direction opposite to that of the transepithelial  $\text{NH}_3$  concentration difference. In the steady state, net ammonium absorption occurs because the rate of active transport of  $\text{NH}_4^+$  from lumen to bath exceeds the rate of backflux of  $\text{NH}_3$  into the tubule lumen.

The unusual capacity of the thick ascending limb to transport  $\text{NH}_4^+$  more rapidly than  $\text{NH}_3$  is reflected in the response of intracellular pH ( $\text{pH}_i$ ) in this segment to ammonium addition. In mouse MTALs studied by *in vitro* perfusion or in tubule suspension (Kikeri, Sun, Zeidel, and Hebert, 1989), and in preliminary studies in the isolated, perfused rat MTAL (Watts and Good, 1990), addition of ammonium to the tubule lumen or to both the lumen and bath resulted in an abrupt intracellular acidification. This  $\text{pH}_i$  response is opposite to that observed in other cell types, which alkalinize when exposed to ammonium due to predominant entry of  $\text{NH}_3$  (Roos and Boron, 1981), and suggests that  $\text{NH}_4^+$  transport may be an important influence on  $\text{pH}_i$  in MTAL cells. The physiologic significance of ammonium as a determinant of  $\text{pH}_i$  in the MTAL is unclear, however, because there have been no reports of the effects of ammonium on steady state  $\text{pH}_i$  in  $\text{HCO}_3^-$ -containing solutions, and no studies have correlated changes in  $\text{pH}_i$  with changes in net ammonium absorption.

Additional uncertainty exists regarding pathways for apical membrane  $\text{NH}_4^+$  transport. Several observations support the view that absorption of  $\text{NH}_4^+$  by the MTAL is a secondary-active process mediated by substitution of  $\text{NH}_4^+$  for  $\text{K}^+$  on the apical membrane  $\text{Na}^+\text{-K}^+\text{-2Cl}^-$  cotransporter. These include inhibition of ammonium absorption by luminal furosemide (Good et al., 1984; Garvin et al., 1988) or an increase in luminal  $\text{K}^+$  concentration (Good, 1987, 1988), and the demonstration that  $\text{NH}_4^+$  could replace  $\text{K}^+$  in supporting bumetanide-sensitive  $\text{Na}^+$  uptake into outer medullary vesicles (Kinne, Kinne-Saffran, Schutz, and Scholermann, 1986). More recently, an important role for uptake of  $\text{NH}_4^+$  via apical membrane  $\text{K}^+$  channels has been suggested. In mouse MTAL suspensions, most of the intracellular acidification induced by ammonium addition was inhibited by  $\text{Ba}^{2+}$ , a  $\text{K}^+$  channel blocker (Kikeri et al., 1989). In addition, when ammonium was added to the lumen of isolated, perfused mouse MTALs, the rate of  $\text{Ba}^{2+}$ -sensitive  $\text{NH}_4^+$  influx (calculated from changes in  $\text{pH}_i$ ) exceeded the rate of furosemide-sensitive influx (Kikeri, Sun, Zeidel, and Hebert, 1992), suggesting that uptake of  $\text{NH}_4^+$  via  $\text{K}^+$  channels may be

<sup>1</sup> In this paper, as in previous papers (Knepper et al., 1989; Good, 1990b), the terms ammonium and total ammonia are used interchangeably to indicate the sum of  $\text{NH}_4^+$  and  $\text{NH}_3$ . When mechanisms of transport are discussed, the chemical formulas  $\text{NH}_4^+$  and  $\text{NH}_3$  are used to indicate the specific chemical species being transported.

the predominant mode of apical  $\text{NH}_4^+$  entry. No studies, however, have examined directly the role of the  $\text{Ba}^{2+}$ -sensitive pathway in transcellular ammonium absorption. Furthermore, Bleich, Schlatter, and Greger (1990) reported that  $\text{K}^+$  channels in excised patches of apical membrane from rat thick ascending limbs did not conduct  $\text{NH}_4^+$ . Thus, the possible contribution of  $\text{NH}_4^+$  uptake via apical  $\text{K}^+$  channels to transcellular ammonium absorption is unclear.

The present study was designed to examine directly relations between ammonium transport and  $\text{pH}_i$  in the isolated, perfused MTAL of the rat. The specific goals were: (a) to assess the role of ammonium as a determinant of steady state  $\text{pH}_i$ ; and examine the effects on  $\text{pH}_i$  of maneuvers that alter the rate of transcellular  $\text{NH}_4^+$  absorption, (b) to identify  $\text{NH}_4^+$  transport pathways across the apical membrane, and (c) to determine the relative contributions of apical membrane  $\text{NH}_4^+$  transport pathways to transcellular ammonium absorption under physiologic (symmetric ammonium) conditions. The results demonstrate that ammonium transport is a critical determinant of steady state  $\text{pH}_i$  in the MTAL and that most or all of transcellular ammonium absorption is mediated by apical membrane  $\text{Na}^+\text{-NH}_4^+\text{-2Cl}^-$  cotransport.  $\text{NH}_4^+$  also permeates a barium-sensitive apical transport pathway but this does not contribute significantly to net ammonium absorption.

## METHODS

### *Isolation of Tissue*

Pathogen-free male Sprague-Dawley rats (50–80 g body weight, Taconic, Germantown, NY) were injected intraperitoneally with furosemide (2 mg) 15 min before being anesthetized with sodium pentobarbital (50–70 mg/kg body weight). The left kidney was cooled in situ by superfusion with ice-cold dissection solution for 1–2 min, and then removed and sliced for tubule dissection. These procedures help to preserve the viability of rat medullary thick ascending limbs in vitro, presumably by reducing oxygen consumption during tissue isolation (Good et al., 1984; Good, 1988). Medullary thick ascending limbs were dissected from the inner stripe of the outer medulla at 10°C in control bath solution (solution 2, Table I), transferred to a bath chamber on the stage of an inverted microscope, and perfused in vitro at 37°C as previously described (Good et al., 1984; Good, 1988). Modifications of the perfusion system for  $\text{pH}_i$  experiments are described below.

### *Solutions*

The composition of control solutions is given in Table I. These basic solutions were modified for individual experimental protocols as described in Results. BCECF-AM (Molecular Probes, Inc., Eugene, OR) was prepared as a 5-mM stock in dimethyl sulfoxide and diluted into bath solution (solution 2) to a final concentration of 20  $\mu\text{M}$ . Nigericin (Sigma Chemical Co., St. Louis, MO) was prepared as a 10 mM stock in ethanol and diluted into calibration solutions (solution 3) to a final concentration of 10  $\mu\text{M}$ .

For experiments involving measurement of  $\text{pH}_i$ , the composition of the perfusate (solution 1) differed from that of the bath (solution 2) in two ways: (a) divalent and organic anions were replaced with chloride to prevent precipitation with luminal barium, and (b) 44 mM NMDGCl was added so that the addition of luminal  $\text{NH}_4^+$  (20 mM) and/or inhibitors (12 mM  $\text{Ba}^{2+}$ , 21 mM  $\text{K}^+$ ) could be accomplished by replacement of  $\text{NMDG}^+$  at constant luminal  $[\text{Na}^+]$  and  $[\text{Cl}^-]$ . The greater osmolality of the perfusate (360 vs 290 mosmol/kg  $\text{H}_2\text{O}$ ) is unlikely to have

influenced our results because: (a) baseline pH<sub>i</sub> measured with the hyperosmotic perfusate (solution 1) did not differ from that measured in separate tubules using an isosmotic perfusate (solution 2 minus albumin), either in the absence [ $7.16 \pm 0.02$ , hyperosmotic ( $n = 6$ ) vs  $7.10 \pm 0.02$ , isosmotic ( $n = 7$ ),  $P = \text{NS}$ ], or presence [ $6.61 \pm 0.03$ , hyperosmotic ( $n = 18$ ) vs  $6.61 \pm 0.02$ , isosmotic ( $n = 8$ ),  $P = \text{NS}$ ] of 4 mM NH<sub>4</sub>Cl; (b) luminal hyperosmolality has no detectable effect on net ammonium absorption rate or transepithelial voltage (see below); (c) changes in lumen osmolality have no effect on MTAL cell volume (Hebert, 1986a); and (d) increases in lumen osmolality similar to those used in the present study have no effect on MTAL shunt conductance or  $P_{\text{Na}}/P_{\text{Cl}}$  permeability ratio (Hebert and Andreoli, 1986). In the net ammonium transport experiments, 10 mM NMDGCl was added to the perfusate (solution 4) to permit equimolar replacement of NMDG<sup>+</sup> with Ba<sup>2+</sup> (see Results). Control rates of net ammonium absorption and transepithelial voltage obtained with the hyperosmotic perfusate

TABLE I  
*Composition of Control Solutions*

	pH <sub>i</sub> experiments			JAm experiments	
	Perfusate (1)	Bath (2)	Calibration (3)	Perfusate (4)	Bath (5)
NaCl	122	120	15	122	120
NaHCO <sub>3</sub>	25	25	—	25	25
K <sub>2</sub> HPO <sub>4</sub>	—	2	2.5	—	2
KCl	4	—	90	4	—
NH <sub>4</sub> Cl	—	—	—	4	4
Na <sub>2</sub> SO <sub>4</sub>	—	1.2	—	—	1.2
CaCl <sub>2</sub>	2	1	2	2	1
Ca(lactate) <sub>2</sub>	—	1	—	—	1
MgCl <sub>2</sub>	1.5	—	1.5	1.5	—
Mg <sub>3</sub> (citrate) <sub>2</sub>	—	0.5	—	—	0.5
HEPES	—	—	25	—	—
NMDGCl	44	—	20	10	—
Glucose	—	5.5	5	5.5	5.5
Albumin	—	0.2*	—	—	0.2*

\*All values are in mM, except Albumin (g/100 ml). *N*-methyl-D-glucammonium chloride (NMDGCl) was made by reacting *N*-methyl-D-glucamine with equimolar HCl. Solutions 1, 2, 4, and 5 were equilibrated with 94% O<sub>2</sub>/6%CO<sub>2</sub> to pH 7.41. Solution 3 was equilibrated with 100% O<sub>2</sub> and titrated to pH 6.2, 6.5, 6.9, 7.3, or 7.8 using NaOH or HCl. Solution 3 also contained 10 μM nigericin. pH<sub>i</sub> and JAm solutions were modified for individual experiments as described in Results.

(Table IV) were similar to values reported previously in this laboratory using an isosmotic perfusate (Good, 1990a, b).

#### *Measurement of Net Ammonium Transport*

MTAL were mounted on concentric glass pipettes and perfused *in vitro* as previously described (Good et al., 1984; Good, 1988, 1990a). The luminal perfusion rate (normalized per unit tubule length) was adjusted to 5–6 nl/min/mm. The tubules were equilibrated for 20–30 min at 37°C and then two or three tubule fluid samples were collected for each experimental period. Total ammonia concentrations and transepithelial voltage were measured as previously described (Good and Vurek, 1983; Good et al., 1984; Good, 1988). Because net fluid transport is absent in rat MTALs (Good et al., 1984; Good, 1992), absolute rates of ammonium

absorption ( $J_{\text{Am}}$ , pmol/min/mm) were calculated as  $J_{\text{Am}} = V([\text{Am}]_0 - [\text{Am}]_i)/L$ , where  $V$  is fluid collection rate (nl/min),  $[\text{Am}]$  is total ammonia concentration (mM) in perfused (o) and collected (i) fluid, and  $L$  is perfused tubule length (mm). A mean total ammonia absorption rate and transepithelial voltage was calculated for each period studied in a given tubule. When control measurements were made at the beginning and end of an experiment, the control values were averaged. Single tubule values (presented in Fig. 5) were averaged to obtain the group means presented in Table IV.

#### Measurement of Intracellular pH

*Tubule perfusion.* Two modifications of the tubule perfusion system were implemented for pH<sub>i</sub> experiments.

(a) Perfusion solutions were delivered to the pipettes via a syringe pump (Harvard Apparatus, Inc., South Natick, MA) connected through a pneumatically activated four-way valve (Beckman-Alex, San Ramon, CA). With this system, one solution is delivered to the perfusion pipettes while a second solution is delivered continuously through a waste line fitted with a length of small diameter glass tubing to equalize fluid pressure in the two lines. Activation of the valve rapidly switches the path of the solutions. The vast majority of fluid delivered to the pipettes exits the rear of the pipette system through a drain port; <0.0001% of the fluid perfuses the tubule lumen. This method results in a smooth and complete exchange of the luminal solution in <2 s, as measured by (a) the time necessary for appearance or disappearance of colored dye, and (b) the time required for the maximal increase in luminal fluorescence after change of the perfusate to one containing BCECF. The perfusion rate for all pH<sub>i</sub> experiments was  $\geq 20$  nl/min to minimize axial changes in luminal fluid composition. All perfusion solutions were delivered through CO<sub>2</sub> impermeable Saran tubing.

(b) A blackened laminar-flow bath chamber (total volume 150  $\mu$ l) was used to minimize tubule vibration and to reduce scattering of excitation and emitted light. Gas-equilibrated bath solutions were delivered through glass lines by hydrostatic pressure at a rate of 2.5–3.5 ml/min and warmed to 37°C by water jackets immediately prior to the chamber. The pH of 25 mM HCO<sub>3</sub><sup>-</sup>, 94% O<sub>2</sub>/6% CO<sub>2</sub> solutions, monitored in the bath chamber with a microcombination pH electrode (Microelectrodes, Inc., Londonderry, NH), was 7.41.

*Fluorescence measurements.* pH<sub>i</sub> was monitored using the fluorescent probe 2',7'-bis(carboxyethyl)-5,6-carboxyfluorescein (BCECF) (Rink, Tsien, and Pozzan, 1982) and an inverted fluorescence microscope (Nikon Diaphot-DMC). After a MTAL was mounted on the pipettes, a rectangular diaphragm was adjusted over a 0.2–0.3 mm length of the tubule and background fluorescence was measured. The tubules were then loaded with dye by exposing the cells for ~15 min at room temperature to bath solution (solution 2, Table I) containing 20  $\mu$ M of the lipid-soluble, acetoxymethyl derivative of BCECF (BCECF-AM). Fresh loading solution was introduced into the bath at regular intervals to maintain tubule oxygenation and bath pH. Loading was continued until the fluorescence intensity was 20–30 $\times$  background at 440 nm excitation. The loading solution was then washed out by initiation of bath flow, and the tubule was equilibrated at 37°C with dye-free bath solution for 10–15 min before experimental measurements.

Excitation light from a 75-W xenon arc lamp was passed through either a 500 nm or 440 nm optical discriminating filter (Omega Optics, Brattleboro, VT). Emitted light was collected through an extended reflectivity dichroic mirror (DR series, Omega), passed through a 530 nm filter (5 nm bandwidth, Omega Optics), and focused onto a photomultiplier tube (Nikon P1). The output of the photomultiplier was directed to a strip-chart recorder (Soltec) for analysis.

Fig. 1, A and B, shows tracings for two pH<sub>i</sub> experiments. Calculated pH<sub>i</sub> values for these experiments are shown in Figs. 3 A and 4 A. Fluorescence intensity at 530 nm was monitored continuously at 500 nm excitation (F500) with brief, intermittent interruptions to measure

intensity at 440 nm (F440). After correction for background, the average of two 500 nm measurements was divided by the intervening 440 nm measurement to obtain the fluorescence excitation ratio (F500/F440), which is  $\text{pH}_i$ -dependent (Rink et al., 1982). A two or three point calibration of intracellular dye was obtained at the end of each experiment (see below) to convert excitation ratios to  $\text{pH}_i$  values. The initial rate of change of  $\text{pH}_i$  ( $\text{dpH}_i/\text{dt}$ ) was determined from the initial slope of the 500 nm tracing measured over the first 4 s after an experimental maneuver. An F440 value for this time period was interpolated from values

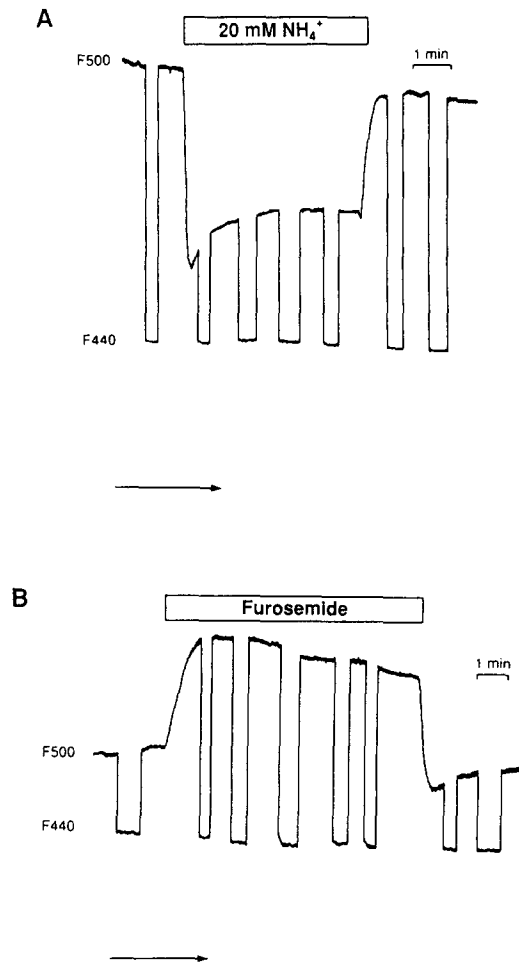


FIGURE 1. Tracings for two  $\text{pH}_i$  experiments. (A) Effect of luminal addition of 20 mM  $\text{NH}_4^+$ . (B) Effect of luminal addition of furosemide ( $10^{-4}$  M) in a tubule perfused and bathed with 4 mM  $\text{NH}_4^+$ . Fluorescence emission intensity at 530 nm was monitored continuously at 500 nm excitation (F500) with brief, intermittent interruptions to measure intensity at 440 nm excitation (F440). Intracellular dye was calibrated at the end of the experiments as described in Methods. F500 and F440 values at selected time points were obtained by correcting total fluorescence intensity for background. Arrows indicate baseline signal obtained with shutter closed.  $\text{pH}_i$  values determined from the F500/F440 ratios are shown in Figs. 3A and 4A. See text for additional details.

measured immediately before and after the experimental maneuver.  $\text{dpH}_i/\text{dt}$  values were calculated as  $\text{dpH}_i/\text{dt} = [(dF500/\text{dt})/(F440)] \times m$ , where  $m$  is the slope of the calibration curve for individual experiments.

Bleaching of the dye was minimized using neutral density filters, by limiting the total time of experiments to 20–30 min, and by illuminating the tissue only when data were obtained. With these procedures, the fluorescence intensity at 440 nm decreased by < 15% over the course of

the experiment and the F500/F440 fluorescence excitation ratio remained constant. Dye leakage was negligible for up to 50 min.

**Calibration.** Intracellular dye was calibrated at the end of each experiment using the high  $[\text{K}^+]$  - nigericin technique of Thomas, Buchsbaum, Zimniak, and Racker, (1979). Tubules were perfused and bathed with a 95 mM  $\text{K}^+$  solution (solution 3, Table I) that contained 10  $\mu\text{M}$  of the  $\text{K}^+/\text{H}^+$  exchanger, nigericin. Under these conditions,  $\text{pH}_i$  approximates the pH of the extracellular solution (Thomas et al., 1979; Chaillet and Boron, 1985). The calibration solution was titrated to selected pH values between 6.2 and 7.8. Fig. 2 summarizes the results of intracellular calibrations obtained in 53 tubules, including eight tubules in which excitation ratios were obtained for each of the five pH values.

In a previous study of  $\text{pH}_i$  using BCECF in rat CTAL, changing  $[\text{K}^+]$  in calibration solutions from 64 to 128 mM at pH 7.3 had no detectable effect on fluorescence-excitation ratios (Krapf, 1988). To assess whether other components of the calibration solution influenced the calibration values, we obtained data in tubules using a solution that contained 50 mM  $\text{K}_2\text{HPO}_4$ , 20 mM HEPES, 0.5 mM Mg citrate, 1.0 mM  $\text{CaCl}_2$ , 1.0 mM Ca lactate, and 10  $\mu\text{M}$  nigericin.

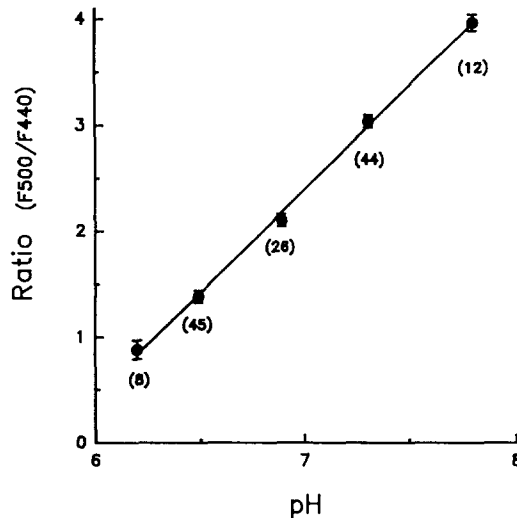


FIGURE 2. Calibration of intracellular dye in rat medullary thick ascending limbs. Filled circles are means  $\pm$  SE obtained from a total of 53 tubules. Numbers in parentheses indicate the numbers of measurements made at each  $\text{pH}_i$ . The line is a first order linear regression fit to the means ( $r^2 = 0.99$ ).

Excitation ratios determined with this solution [ $1.40 \pm 0.02$  at pH 6.5 ( $n = 9$ ) and  $3.00 \pm 0.02$  at pH 7.3 ( $n = 9$ )], were similar to values obtained with solution 3 (Fig. 2).

#### Statistical Analysis

Results of the  $\text{pH}_i$  experiments were evaluated by paired  $t$  test, unpaired  $t$  test, or analysis of variance with Newman-Kuels' multiple range test, as appropriate. In ammonium transport experiments, differences between means were evaluated using the paired  $t$  test. In all cases,  $P < 0.05$  was regarded as statistically significant.

## RESULTS

#### Effects of Luminal Ammonium Addition on $\text{pH}_i$

The effects on  $\text{pH}_i$  of adding ammonium to the tubule lumen are shown in Table II (mean values) and Fig. 3 (single experiments). In the absence of ammonium

(solutions 1 and 2, Table I), the initial intracellular pH was  $7.16 \pm 0.02$  (Table II A). Addition of 20 mM ammonium to the luminal perfusate (20 mM  $\text{NH}_4^+$  replaced 20 mM NMDG<sup>+</sup>) caused an abrupt intracellular acidification (Figs. 1 A and 3 A) that occurred at an initial rate of  $11.1 \pm 1.0$  U/min (Table II A).  $\text{pH}_i$  recovered slightly following the initial acidifying spike (Figs. 1 A and 3 A). However, steady state  $\text{pH}_i$  in the presence of luminal ammonium ( $6.67 \pm 0.04$ ) was significantly lower than in the absence of ammonium. The steady state  $\text{pH}_i$  fell by  $0.52 \pm 0.04$  U with luminal 20 mM ammonium addition ( $\Delta\text{pH}_i$ , Table II A) and remained stable for up to 20 min. After removal of ammonium,  $\text{pH}_i$  recovered rapidly to its initial control value (Figs. 1 A and 3 A) ( $\text{pH}_i$  after recovery =  $7.12 \pm 0.03$ ,  $n = 6$ ).

The acidification of MTAL cells in response to luminal ammonium addition indicates that  $\text{NH}_4^+$  is transported into the cells at a rate that exceeds the influx of  $\text{NH}_3$ . The role of  $\text{Na}^+ \text{-} \text{NH}_4^+ \text{-} 2\text{Cl}^-$  cotransport in apical  $\text{NH}_4^+$  uptake was assessed by

TABLE II  
Effects of Luminal Ammonium Addition on  $\text{pH}_i$

	$\text{pH}_i$ , U		$\text{dpH}_i/\text{dt}$	$\Delta\text{pH}_i$
	Initial	20 mM $\text{NH}_4^+$		
(A) Control (6)	7.16	6.67	11.1	0.52
	$\pm 0.02$	$\pm 0.04$	$\pm 1.0$	$\pm 0.04$
(B) Furosemide (5), 0.1 mM	7.07	6.71 <sup>‡</sup>	3.6* <sup>‡</sup>	0.35* <sup>‡</sup>
	$\pm 0.04$	$\pm 0.04$	$\pm 0.6$	$\pm 0.03$
(C) Barium (5), 12 mM	7.20	6.83* <sup>‡</sup>	4.6* <sup>‡</sup>	0.38* <sup>‡</sup>
	$\pm 0.03$	$\pm 0.07$	$\pm 0.4$	$\pm 0.04$
(D) Furosemide + barium (5)	7.19	7.06*	0.3*	0.13*
	$\pm 0.04$	$\pm 0.05$	$\pm 0.1$	$\pm 0.03$

Values are means  $\pm$  SE. Numbers in parentheses are numbers of tubules.  $\text{dpH}_i/\text{dt}$ , initial rate of cell acidification after luminal  $\text{NH}_4^+$  addition, calculated from the initial deflection of the 500-nm tracing.  $\Delta\text{pH}_i$ , absolute change in steady state  $\text{pH}_i$  after luminal  $\text{NH}_4^+$  addition. Composition of solutions is given in Methods/Results. Results were analyzed by ANOVA with Newman-Keuls' multiple range test. \* $P < 0.05$  vs control; <sup>‡</sup> $P < 0.05$  vs furosemide + barium. All  $\Delta\text{pH}_i$  values differ significantly from zero (paired  $t$  test), indicating  $\text{pH}_i$  with 20 mM  $\text{NH}_4^+$  significantly less than  $\text{pH}_i$  initial.

adding 20 mM ammonium to the tubule lumen in the presence of  $10^{-4}$  M luminal furosemide (Table II B and Fig. 3 B). Furosemide reduced the initial rate of acidification by 70% and decreased the fall in steady state  $\text{pH}_i$  by 35%. However, furosemide did not completely prevent the intracellular acidification, indicating the presence of a second, furosemide-insensitive pathway for apical  $\text{NH}_4^+$  entry.

The effects on  $\text{pH}_i$  of adding 20 mM ammonium to the tubule lumen in the presence of 12 mM luminal barium (12 mM  $\text{BaCl}_2$  replaced 24 mM NMDGCl) are shown in Table II C and Fig. 3 C.<sup>2</sup>  $\text{Ba}^{2+}$  reduced the initial rate of acidification by 59% and the fall in steady state  $\text{pH}_i$  by 30% compared with control values.

<sup>2</sup> This concentration of  $\text{Ba}^{2+}$  was chosen based on previous studies demonstrating that luminal  $\text{Ba}^{2+}$  concentrations of 10–20 mM were required for maximal blockade of transcellular conductance in the mouse MTAL (Hebert and Andreoli, 1986).



The inhibitory effects of barium could be due either to direct inhibition of  $\text{NH}_4^+$  entry (e.g., by block of apical  $\text{K}^+$  channels) or to a secondary effect of barium to inhibit  $\text{NH}_4^+$  entry via  $\text{Na}^+$ - $\text{NH}_4^+$ - $2\text{Cl}^-$  cotransport (see Discussion). To assess these possibilities, we examined whether the inhibitory effects of furosemide and barium were additive. The effects on  $\text{pH}_i$  of adding 20 mM ammonium to the tubule lumen in the presence of both  $10^{-4}$  M furosemide and 12 mM barium are shown in Table

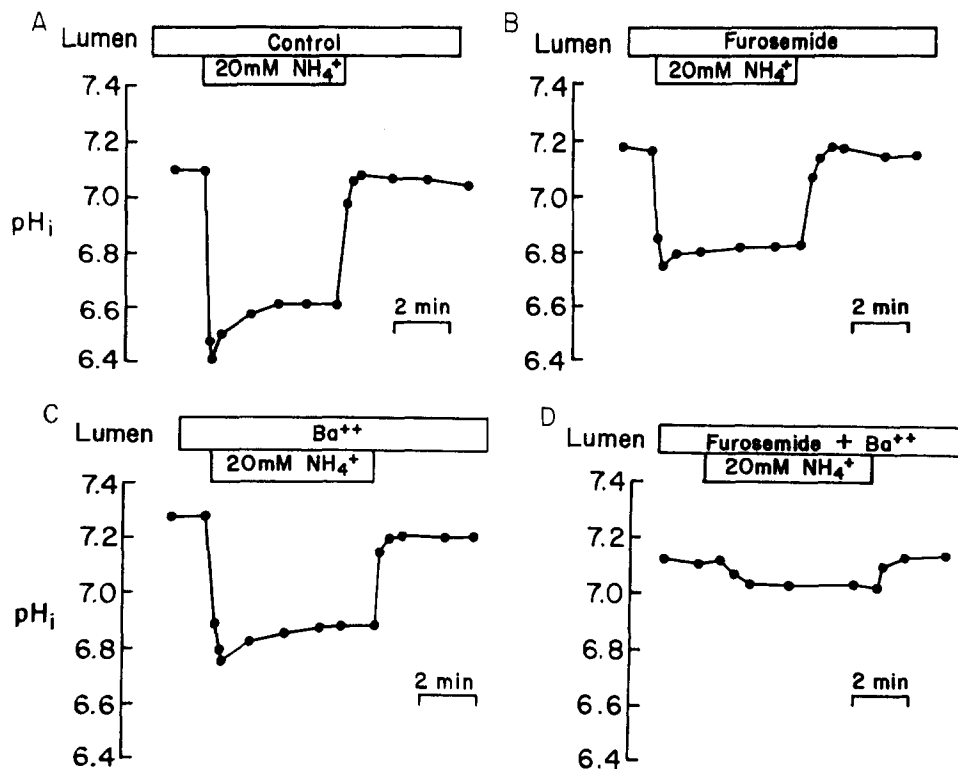


FIGURE 3. Effects of luminal addition of 20 mM  $\text{NH}_4^+$  on  $\text{pH}_i$  in MTAL. Each panel shows results of a single experiment. (A)  $\text{NH}_4^+$  added to control perfusate (fluorescence tracing shown in Fig. 1A). (B–D)  $\text{NH}_4^+$  added to control perfusate in the presence of  $10^{-4}$  M luminal furosemide (B), 12 mM luminal barium (C), or  $10^{-4}$  M furosemide plus 12 mM barium (D). Filled circles are single  $\text{pH}_i$  values obtained from F500/F440 ratios along the fluorescence tracings. Lines are drawn by eye. Composition of all solutions is given in Methods/Results. Mean  $\text{pH}_i$  values are in Table II.

II D and Fig. 3 D. The combination of furosemide plus barium inhibited the cell acidification nearly completely, reducing  $\text{dpH}_i/\text{dt}$  by 97% and  $\Delta\text{pH}_i$  by 75% compared with control values. With furosemide plus barium,  $\text{dpH}_i/\text{dt}$  and  $\Delta\text{pH}_i$  also were significantly less than values observed with either furosemide or barium alone (Table II). These results are consistent with entry of  $\text{NH}_4^+$  through both furosemide- and barium-sensitive pathways, presumably apical membrane  $\text{Na}^+$ - $\text{NH}_4^+$ - $2\text{Cl}^-$  cotransport

and  $K^+$  channels. Note, however, that even in the presence of both furosemide and barium, the luminal addition of ammonium resulted in a significant decrease in  $pH_i$  (Table II D, Fig. 3 D). Thus, mechanisms for  $NH_4^+$ -dependent cell acidification persist when the two pathways for apical  $NH_4^+$  entry are inhibited.

*Effect of Symmetric Ammonium Addition on  $pH_i$*

To assess whether the pronounced effect of luminal ammonium addition on  $pH_i$  may be of physiologic significance, further experiments were performed in which a physiologic concentration of ammonium (4 mM) was added to both the luminal and peritubular solutions (4 mM  $NH_4^+$  replaced 4 mM NMDG<sup>+</sup> in perfusate; 4 mM  $NH_4Cl$  was added to bath). In MTALs studied at pH 7.4 in 25 mM  $HCO_3^-$  solutions in the absence of ammonium (solutions 1 and 2, Table I), intracellular pH was  $7.16 \pm 0.02$  ( $n = 6$ ). In contrast, in tubules studied under identical conditions at the same

TABLE III  
*Effects of Inhibitors on  $pH_i$  in Symmetric Ammonium Solutions*

	$pH_i$ , U		$dpH_i/dt$	$\Delta pH_i$
	Initial	Inhibitor		
(A) Furosemide (5), 0.1 mM	6.55	6.96	<i>U/min</i> 0.82	<i>U</i> 0.41
	$\pm 0.02$	$\pm 0.03$	$\pm 0.14$	$\pm 0.03$
(B) Barium (7), 12 mM	6.64	7.02	0.32*	0.38
	$\pm 0.02$	$\pm 0.02$	$\pm 0.05$	$\pm 0.02$
(C) High $K^+$ (6)	6.62	6.96	0.89	0.34
	$\pm 0.06$	$\pm 0.06$	$\pm 0.09$	$\pm 0.02$

Values are means  $\pm$  SE. Tubules were perfused and bathed initially in control solutions (solutions 1 and 2, Table I) containing 4 mM  $NH_4^+$  and then inhibitor was added to the luminal perfusate. In high  $K^+$  experiments, luminal  $[K^+]$  was increased from the control value of 4 mM to 25 mM.  $dpH_i/dt$ , initial rate of cell alkalinization following addition of inhibitor, calculated from the initial deflection of the 500 nm tracing.  $\Delta pH_i$ , absolute change in steady state  $pH_i$  after addition of inhibitor. All  $\Delta pH_i$  values differ significantly from zero, indicating  $pH_i$  with inhibitor significantly greater than  $pH_i$  initial. Numbers in parentheses and statistical analysis as in Table II. \* $P < 0.01$  vs either furosemide or high  $K^+$ .

extracellular pH, but with 4 mM  $NH_4^+$  in the perfusate and bath,  $pH_i$  was reduced markedly to  $6.61 \pm 0.02$  ( $n = 18$ ) ( $P < 0.001$  vs zero ammonium). In 4 mM  $NH_4^+$  solutions,  $pH_i$  was stable for up to 20 min. Thus, the presence of ammonium is a critical determinant of steady state  $pH_i$  in the rat MTAL.

*Effects of Inhibitors on  $pH_i$  and Net Ammonium Transport in Symmetric Ammonium Solutions*

The experiments with luminal ammonium addition (Table II, Fig. 3) can identify pathways through which ammonium may be transported; however, they do not clarify the roles of the furosemide- and barium-sensitive pathways in net ammonium absorption under physiologic conditions in which ammonium is present on both sides of the tubule. To address this question, two different experimental approaches were

used, one involving the measurement of  $\text{pH}_i$  and the other involving measurement of net ammonium fluxes.

**Intracellular pH.** To assess apical  $\text{NH}_4^+$  uptake under symmetric ammonium conditions,  $\text{pH}_i$  was monitored in tubules that were perfused and bathed continuously with 4 mM  $\text{NH}_4^+$  and then either furosemide or barium was added to the luminal

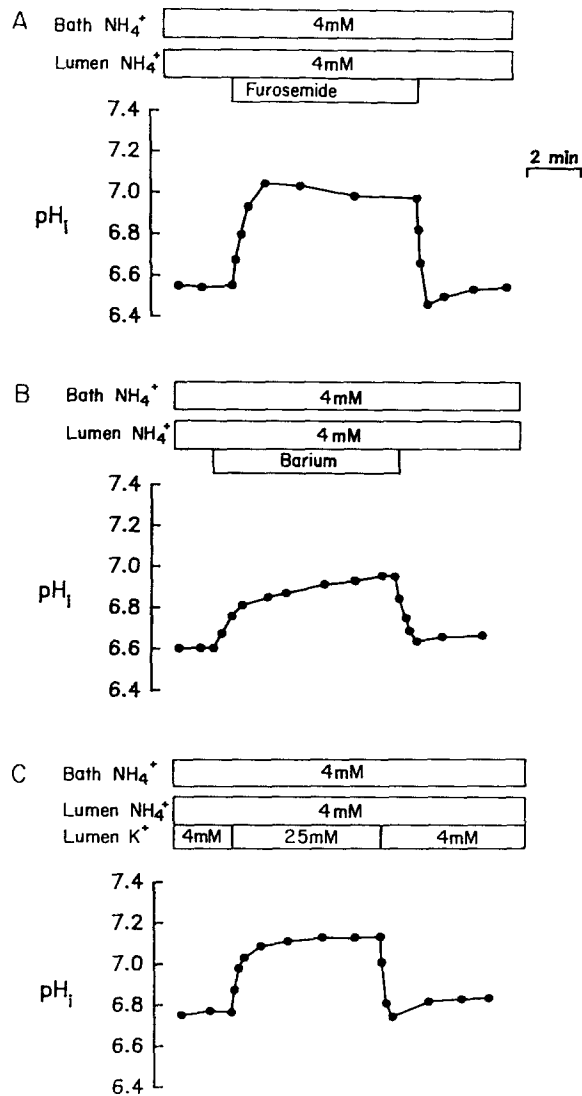


FIGURE 4. Effects of inhibitors on  $\text{pH}_i$  in the presence of  $\text{NH}_4^+$ . Each panel shows results of a single experiment. MTAL were perfused and bathed continuously with 4 mM  $\text{NH}_4^+$  and then either  $10^{-4}$  M furosemide (A) or 12 mM barium (B) was added to the luminal fluid (fluorescence tracing for A experiment shown in Fig. 1 B). (C) Shows the effect of increasing luminal  $\text{K}^+$  concentration from 4 to 25 mM. Filled circles and lines as in Fig. 3. Composition of solutions is given in Methods/Results. Mean  $\text{pH}_i$  values are in Table III.

perfusate. The results of these experiments are shown in Table III and Fig. 4. The initial mean steady state  $\text{pH}_i$  with 4 mM  $\text{NH}_4^+$  in perfusate and bath ranged from 6.55 to 6.64 (Table III). Addition of  $10^{-4}$  M furosemide to the tubule lumen caused an abrupt intracellular alkalinization ( $\text{dpH}_i/\text{dt} = 0.82 \pm 0.14$  U/min) and increased the

mean steady state  $\text{pH}_i$  from 6.55 to 6.96 (Table III A, Figs. 1 B and 4 A). In separate experiments, luminal furosemide had no significant effect on  $\text{pH}_i$  in tubules studied under identical conditions in the absence of ammonium ( $7.05 \pm 0.04$ , control vs  $7.05 \pm 0.03$ , furosemide,  $n = 6$ ;  $P = \text{NS}$ ). Thus, the cell alkalization was dependent on the presence of ammonium and likely was due to inhibition of apical ammonium entry via  $\text{Na}^+\text{-NH}_4^+\text{-2Cl}^-$  cotransport. The cells acidified rapidly after removal of furosemide (Figs. 1 B and 4 A), consistent with restoration of apical  $\text{NH}_4^+$  entry.

Fig. 4 B and Table III B show the results of experiments in which 12 mM barium was added to the lumen of tubules perfused and bathed with 4 mM  $\text{NH}_4^+$ . The addition of barium caused steady-state  $\text{pH}_i$  to increase from  $6.64 \pm 0.02$  to  $7.02 \pm 0.02$  (Table III B). However, in contrast to the rapid alkalization observed with

TABLE IV  
Effect of Luminal Furosemide or Barium on Net Ammonium Absorption

	V	[Am], mM		JAm	$V_{\text{TE}}$
		perfused	collected		
(A) Control	6.2	4.0	2.2*	11.3	2.5
	$\pm 0.2$	$\pm 0.03$	$\pm 0.05$	$\pm 0.6$	$\pm 0.5$
Furosemide	5.9	4.0	3.9	0.7	-0.5
	$\pm 0.1$	$\pm 0.03$	$\pm 0.07$	$\pm 0.4$	$\pm 0.2$
P	NS	NS	<0.001	<0.005	<0.005
(B) Control	5.9	4.0	1.8*	12.8	4.3
	$\pm 0.6$	$\pm 0.05$	$\pm 0.12$	$\pm 2.0$	$\pm 1.0$
Barium	6.1	4.0	2.2*	11.0	1.4
	$\pm 0.6$	$\pm 0.04$	$\pm 0.23$	$\pm 2.4$	$\pm 0.3$
P	NS	NS	<0.05	<0.05	<0.05

Values are means  $\pm$  SE. Number of experiments equals four with furosemide and four with barium. Composition of control perfusion and bath solutions is given in Table I (solutions 4 and 5). In series A,  $1 \times 10^{-4}$  M furosemide was added to the perfusate; in series B, 10 mM  $\text{BaCl}_2$  replaced 10 mM NMDGCl. Mean tubule length was  $0.52 \pm 0.02$  mm with furosemide and  $0.55 \pm 0.02$  mm with barium. V, fluid collection rate; [Am], total ammonia concentration; JAm, absolute rate of total ammonia absorption;  $V_{\text{TE}}$ , transepithelial voltage, oriented lumen positive with respect to bath. [Am] in bath was  $4.0 \pm 0.03$  mM. P values are for control vs furosemide or barium (paired *t* test). \*Collected [Am] significantly different from perfused.

furosemide, adding barium to the lumen resulted in a slow alkalization that occurred at an initial rate only 39% of that observed with furosemide (Table III). Because inhibition of apical  $\text{K}^+$  channels by  $\text{Ba}^{2+}$  is virtually complete within  $\sim 2$  s (Greger and Schlatter, 1983), this slow  $\text{pH}_i$  response suggests that there is not rapid entry of  $\text{NH}_4^+$  through the barium-sensitive pathway under symmetric ammonium conditions. In the absence of  $\text{NH}_4^+$ , adding 12 mM  $\text{Ba}^{2+}$  to the perfusate caused a small intracellular alkalization ( $\Delta\text{pH}_i = 0.08 \pm 0.02$ ,  $n = 4$ ,  $P < 0.05$ ). Thus, the slow response of  $\text{pH}_i$  in the presence of  $\text{NH}_4^+$  was not due to the presence of an opposing,  $\text{NH}_4^+$ -independent action of  $\text{Ba}^{2+}$  to cause cell acidification.

*Net ammonium absorption.* The effects of furosemide and barium on net ammonium absorption in MTALs perfused and bathed with 4 mM  $\text{NH}_4^+$  are shown in Table IV and Fig. 5. Consistent with previous experiments performed at slow flow rates

(Good et al., 1984), adding  $10^{-4}$  M furosemide to the tubule lumen abolished net ammonium absorption and reduced the transepithelial voltage to near zero. Both effects were reversible. In contrast, adding 10 mM barium to the lumen caused only a small inhibition of ammonium absorption, reducing the mean transport rate from 12.8 to 11.0 pmol/min/mm. It is unlikely that uptake of  $\text{NH}_4^+$  via the  $\text{Na}^+\text{-K}^+\text{-2Cl}^-$  cotransporter was increased with luminal barium because barium inhibits furosemide-sensitive chloride absorption (see Discussion). Thus, these findings are consistent with the conclusions drawn from the preceding  $\text{pH}_i$  experiments, namely, that entry of  $\text{NH}_4^+$  through the barium-sensitive pathway is not an important mechanism for ammonium absorption under symmetric ammonium conditions, and that most or all of transcellular ammonium absorption occurs through a furosemide-sensitive pathway. Luminal  $\text{Ba}^{2+}$  reduced the transepithelial voltage by 67% (Table IV B).

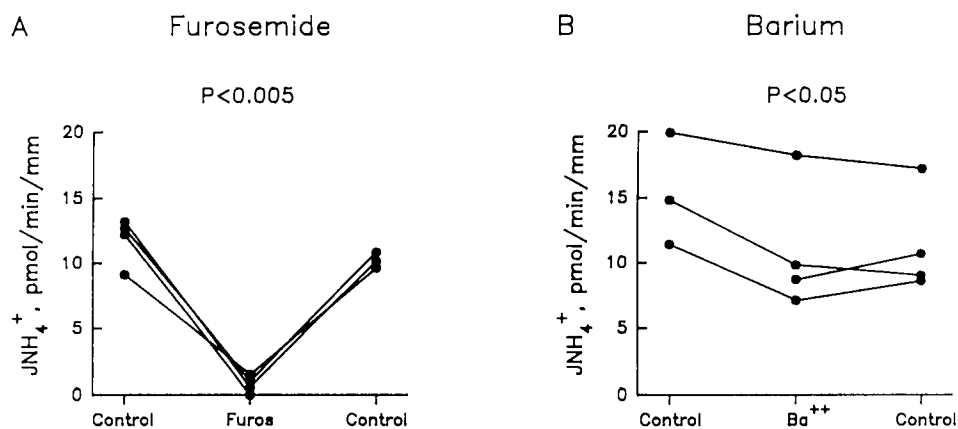


FIGURE 5. Effect of furosemide ( $10^{-4}$  M) or barium (10 mM) in the perfusate on total ammonia absorption by the MTAL. The perfusion and bath solutions contained 4 mM  $\text{NH}_4^+$  (solutions 4 and 5, Table I). Filled circles are mean values for single tubules; lines connect paired measurements made in the same tubule.  $P$  values are for paired  $t$  test. Mean values are in Table IV.

#### *Effect of Luminal $\text{K}^+$ Concentration on $\text{pH}_i$ in Symmetric Ammonium Solutions*

In addition to furosemide, another maneuver that markedly inhibits active  $\text{NH}_4^+$  absorption in the MTAL is an increase in luminal  $\text{K}^+$  concentration (Good, 1987, 1988). This inhibition is believed to result from competition between  $\text{K}^+$  and  $\text{NH}_4^+$  on the apical membrane  $\text{Na}^+\text{-K}^+\text{-2Cl}^-$  cotransporter (Good, 1988). If this explanation is correct, then increasing luminal  $[\text{K}^+]$  in the presence of ammonium should alkalinize MTAL cells in a manner similar to that observed with furosemide. Fig. 4 C and Table III C show the effects on  $\text{pH}_i$  of increasing luminal  $\text{K}^+$  concentration from 4 to 25 mM (21 mM  $\text{K}^+$  replaced 21 mM  $\text{NMDG}^+$ ) in MTAL perfused and bathed with 4 mM  $\text{NH}_4^+$ . Increasing the luminal  $\text{K}^+$  concentration resulted in an abrupt intracellular alkalinization (to  $\text{pH}_i$  7.0) that occurred at a rapid rate ( $\text{dpH}_i/\text{dt} = 0.89 \pm 0.09$  U/min) similar to that observed with furosemide. In three additional tubules,

increasing luminal  $[K^+]$  from 4 to 25 mM in the absence of  $NH_4^+$  caused  $pH_i$  to increase only by  $0.08 \pm 0.01$  ( $pH_i = 7.15 \pm 0.01$ , 4  $K^+$  vs  $7.23 \pm 0.01$ , 25  $K^+$ ;  $P < 0.05$ ).

#### DISCUSSION

In contrast to the general observation that  $NH_3$  traverses cell membranes much more rapidly than  $NH_4^+$ , transepithelial ammonium absorption in the MTAL occurs by active transport of  $NH_4^+$  against a concentration difference for  $NH_3$  (Good et al., 1984; Good, 1988; Knepper et al., 1989). The present study was designed to examine the influence of ammonium transport on  $pH_i$  in the isolated, perfused MTAL of the rat and to identify the apical membrane transport pathways responsible for transcellular  $NH_4^+$  absorption. The results demonstrate that (a) ammonium transport is a major determinant of  $pH_i$  in the MTAL, with transcellular ammonium absorption markedly acidifying the cells and maneuvers that inhibit  $NH_4^+$  absorption causing intracellular alkalinization, (b) most or all of transcellular  $NH_4^+$  absorption is mediated by apical membrane  $Na^+ - NH_4^+ - 2Cl^-$  cotransport, and (c)  $NH_4^+$  also permeates a barium-sensitive apical membrane transport pathway but this is not a quantitatively important pathway for ammonium absorption. The bases for these conclusions are discussed below. The physiologic significance of MTAL ammonium absorption has been discussed previously (Knepper et al., 1989; Good and Knepper, 1990).

#### *$NH_4^+$ Transport as a Determinant of $pH_i$*

Addition of ammonium to the lumen of the MTAL resulted in an abrupt and sustained intracellular acidification (Table II, Figs. 1 A and 3), indicating that  $NH_4^+$  is transported into the cell across the apical membrane more rapidly than  $NH_3$ . These apical membrane transport properties are consistent with the results of previous transepithelial transport studies in which active transport of  $NH_4^+$  predominated over transport of  $NH_3$  to result in net ammonium absorption (Good et al., 1984; Good, 1988; Garvin et al., 1988).

An effect of ammonium addition to cause intracellular acidification was observed previously by Kikeri et al. (1989) in mouse MTALs studied in  $HCO_3^-$ -free solutions, conditions in which a reduced cell buffering capacity and/or a diminished contribution of  $HCO_3^-$ -dependent transporters to  $pH_i$  regulation may have magnified the change in  $pH_i$  in response to ammonium addition. Those concerns were obviated in the present study since all  $pH_i$  measurements were made in the presence of 25 mM  $HCO_3^-$  and 6%  $CO_2$ , conditions similar to those present in the renal medulla in vivo (DuBose, Lucci, Hogg, Pucacco, Kokko, and Carter, 1983). Thus, the pronounced intracellular acidification observed with ammonium addition indicates that transcellular ammonium transport results in a large and continuous net acid load to the cell. Mechanisms for  $pH_i$  regulation were evident in the slight recovery of  $pH_i$  following the initial acidifying spike (Fig. 3 A) and in the recovery of  $pH_i$  to its initial control value following ammonium removal (Figs. 1 A and 3). The fact that exposure to ammonium results in a large and sustained fall in  $pH_i$  indicates that the acid-loading effects of ammonium transport predominate over the mechanisms for  $pH_i$  regulation, thereby resetting the steady state  $pH_i$  to a lower value.

The mechanisms by which ammonium transport results in intracellular acidification have not been identified; however, a few points are noteworthy. First, uptake of  $\text{NH}_4^+$  into the cell by itself cannot account for the pronounced cell acidification. This is because the cell pH is  $\sim 2$  pH units below the  $\text{pK}_a$  for the ammonium buffer reaction ( $\text{pK}_a \approx 9.0$ ). As a result, only  $\sim 1\%$  of the  $\text{NH}_4^+$  entering the cells would release a proton, resulting in a negligibly small cell acid load that could readily be neutralized by the cell buffers.<sup>3</sup> Consequently, mechanisms in addition to apical  $\text{NH}_4^+$  entry must play a role in the intracellular acidification. Rapid entry of  $\text{NH}_4^+$  across the apical membrane coupled with efflux of  $\text{NH}_3$  across the basolateral membrane (Kikeri et al., 1989) would result in the net deposition of protons inside the cell and could contribute to the fall in  $\text{pH}_i$ . Other mechanisms, such as effects of ammonium on  $\text{H}^+$  or  $\text{HCO}_3^-$  transporters or on metabolic acid production also may contribute to the ammonium-induced cell acidification.

The physiologic importance of ammonium as a determinant of  $\text{pH}_i$  is most evident in the experiments with symmetric ammonium solutions. In vivo, the MTAL is exposed to millimolar concentrations of ammonium due to the high concentrations of ammonium generated in the renal medulla by countercurrent multiplication (Knepper et al., 1989; Good and Knepper, 1990). The ammonium concentration used in the present experiments (4 mM) represents a reasonable estimate of the concentration expected to surround the MTAL of the rat in vivo (Good et al., 1984). In tubules studied with 4 mM  $\text{NH}_4^+$  in perfusate and bath, the mean  $\text{pH}_i$  was more than 0.5 pH U less than that in tubules studied under the same conditions in the absence of ammonium, even though the extracellular fluid pH was identical (7.4) in the two groups. In addition, luminal furosemide had no effect on  $\text{pH}_i$  in the absence of ammonium but caused a marked intracellular alkalinization in MTALs perfused and bathed with 4 mM  $\text{NH}_4^+$ . Increasing the luminal  $[\text{K}^+]$  also caused a pronounced intracellular alkalinization that was four times greater in the presence of ammonium than in its absence. As discussed below, both furosemide and increasing luminal  $[\text{K}^+]$  increase  $\text{pH}_i$  by reducing apical  $\text{NH}_4^+$  uptake via  $\text{Na}^+ \text{-} \text{NH}_4^+ \text{-} 2\text{Cl}^-$  cotransport, thereby diminishing the intracellular acid load that results from transcellular ammonium absorption. Thus, the extent to which factors that regulate  $\text{Na}^+ \text{-} \text{K}^+ \text{-} 2\text{Cl}^-$  cotransport activity influence  $\text{pH}_i$  depends critically on the presence or absence of ammonium. Furthermore, as a result of its influence on  $\text{pH}_i$ , ammonium may secondarily affect other important cellular processes in the MTAL that may be  $\text{pH}_i$ -dependent, such as  $\text{HCO}_3^-$  reabsorption (Good, 1992), volume regulation (Hebert, 1986b), NaCl reabsorption (Wingo, 1986), or  $\text{K}^+$  transport (Oberleithner, Kersting, and Hunter, 1988; Guggino, Oberleithner, and Giebisch, 1988; Bleich et al., 1990; Kikeri et al., 1992).

#### *Apical $\text{NH}_3$ Transport*

Luminal ammonium addition did not result in intracellular alkalinization even when apical  $\text{NH}_4^+$  entry was inhibited with furosemide and barium (Fig. 3 D). This

<sup>3</sup> Assuming as an upper limit a steady state intracellular  $[\text{NH}_4^+]$  of 50–80 mmol/l, the intracellular  $[\text{H}^+]$  at chemical equilibrium (due to dissociation of  $\text{NH}_4^+$ ) would be 0.7 to 1.0 mmol/l at  $\text{pH}_i$  7.15. In comparison, the total intracellular buffering power of rat MTAL cells at  $\text{pH}_i$  7.15 is 85 mmol/l/pH unit (B. Watts and D. Good, unpublished data). Thus, the change in  $\text{pH}_i$  due to  $\text{H}^+$  generated by dissociation of  $\text{NH}_4^+$  would be immeasurably small ( $\sim 0.01$  U).

observation was reported previously in the mouse MTAL, and was taken as evidence that the apical membrane was impermeable to  $\text{NH}_3$  (Kikeri et al., 1989). However, both in that study and in the present study (Table II *D*, Fig. 3 *D*), adding ammonium to the lumen in the presence of furosemide and barium caused  $\text{pH}_i$  to decrease significantly by  $\sim 0.15$  U. Thus, mechanisms for  $\text{NH}_4^+$ -induced cell acidification were still operational despite the presence of the inhibitors, and may have masked an effect of apical  $\text{NH}_3$  entry to cause intracellular alkalization. Other factors may complicate the detection of cell alkalization due to apical  $\text{NH}_3$  entry, including rapid efflux of  $\text{NH}_3$  out of the cell due to a basolateral membrane surface area  $\sim 13\times$  greater than the apical membrane surface area (Kone, Madsen, and Tisher, 1984), which minimizes the amount of intracellular  $\text{NH}_3$  available to bind protons. Thus, further work is needed to quantify the apical membrane  $\text{NH}_3$  permeability of the MTAL.

#### *Pathways for Apical Membrane $\text{NH}_4^+$ Transport*

The transport pathways responsible for apical  $\text{NH}_4^+$  uptake were assessed by examining the ability of inhibitors to attenuate the intracellular acidification that results from apical uptake and transcellular absorption of  $\text{NH}_4^+$ . A potential limitation of this approach is that processes other than apical  $\text{NH}_4^+$  uptake may contribute to changes in  $\text{pH}_i$ . This concern was minimized in the present study by (a) determining the effects of inhibitors in both the absence and presence of ammonium to assess  $\text{pH}_i$  effects unrelated to ammonium transport, (b) studying the inhibitors using two different experimental protocols (luminal  $\text{NH}_4^+$  addition and symmetric  $\text{NH}_4^+$ ), and (c) correlating results of the  $\text{pH}_i$  experiments with direct measurements of the net ammonium flux.

#### *Furosemide-sensitive Pathway: $\text{Na}^+$ - $\text{NH}_4^+$ - $2\text{Cl}^-$ Cotransport*

Previous studies have suggested that  $\text{NH}_4^+$  absorption by the MTAL is mediated by substitution of  $\text{NH}_4^+$  for  $\text{K}^+$  on the apical membrane  $\text{Na}^+$ - $\text{K}^+$ - $2\text{Cl}^-$  cotransporter (Good et al., 1984; Kinne et al., 1986; Good, 1988; Knepper et al., 1989). The role of the cotransporter in apical  $\text{NH}_4^+$  uptake was assessed in the present study by examining the effects on net ammonium absorption and  $\text{pH}_i$  of  $10^{-4}$  M luminal furosemide, a concentration that inhibits  $\text{Na}^+$ - $\text{K}^+$ - $2\text{Cl}^-$  cotransport virtually completely in TALs (Greger, 1985). Several observations demonstrate that apical  $\text{NH}_4^+$  entry occurs via the cotransporter: (a) furosemide inhibited by 70% the initial rate of cell acidification in response to luminal ammonium addition, (b) furosemide abolished net ammonium absorption in tubules perfused and bathed with 4 mM  $\text{NH}_4\text{Cl}$ , and (c) addition of furosemide under symmetric ammonium conditions caused a rapid and sustained intracellular alkalization that was not observed when ammonium was absent from the experimental solutions. In symmetric ammonium solutions, the steady state  $\text{pH}_i$  increased with furosemide to a value similar to that observed in tubules studied in the absence of ammonium, consistent with the effect of furosemide to abolish the net ammonium absorptive flux. Taken together, these results indicate that virtually all of transcellular ammonium absorption is mediated by apical membrane  $\text{Na}^+$ - $\text{NH}_4^+$ - $2\text{Cl}^-$  cotransport, and that uptake of  $\text{NH}_4^+$  via the cotransporter is responsible for the intracellular acid loading that accompanies transcellular ammonium transport.



In rat MTALs perfused and bathed *in vitro* with 4 mM  $\text{NH}_4\text{Cl}$ , increasing the luminal  $\text{K}^+$  concentration over the physiologic range (4–24 mM) markedly inhibited active  $\text{NH}_4^+$  absorption (Good, 1987, 1988). The present study demonstrates that the same increase in luminal  $[\text{K}^+]$  also causes a rapid and pronounced intracellular alkalization that mimics that observed with furosemide (Fig. 4). The rapid alkalization is unlikely to have been the result of an effect of increasing  $[\text{K}^+]$  to cause membrane depolarization because (a) increasing luminal  $[\text{K}^+]$  and adding luminal furosemide caused virtually identical cell alkalization but have opposite effects on membrane voltage (Greger, Schlatter, and Lang, 1983; Greger and Schlatter, 1983), and (b) addition of luminal barium, another maneuver that causes rapid membrane depolarization (Greger and Schlatter, 1983), did not reproduce either the rapid increase in  $\text{pH}_i$  or the marked inhibition of  $\text{NH}_4^+$  absorption observed with increasing luminal  $[\text{K}^+]$ . Thus, the effects of potassium to inhibit active  $\text{NH}_4^+$  absorption and markedly increase  $\text{pH}_i$  are most likely the result of competitive inhibition of  $\text{NH}_4^+$  uptake by  $\text{K}^+$  on the apical membrane  $\text{Na}^+\text{-NH}_4^+(\text{K}^+)\text{-2Cl}^-$  cotransporter.

#### *Barium-sensitive Pathway*

Addition of ammonium to the tubule lumen resulted in an appreciable intracellular acidification even when the  $\text{Na}^+\text{-K}^+\text{-2Cl}^-$  cotransporter was blocked with furosemide (Fig. 3). The furosemide-insensitive acidification was inhibited by luminal  $\text{Ba}^{2+}$ , an inhibitor of the apical membrane  $\text{K}^+$  conductance that serves to recycle  $\text{K}^+$  taken up by the  $\text{Na}^+\text{-K}^+\text{-2Cl}^-$  cotransporter (Greger, 1985). Our results do not rule out the presence of a barium-sensitive  $\text{NH}_4^+$  transport pathway other than the apical  $\text{K}^+$  channel. However,  $\text{NH}_4^+$  has been shown to permeate  $\text{K}^+$ -selective channels in a number of different cell types (Knepper et al., 1989). Thus, the barium-sensitive component of  $\text{NH}_4^+$  uptake presumably reflects transport of  $\text{NH}_4^+$  through apical membrane  $\text{K}^+$  channels. This view is consistent with previous findings in the mouse MTAL (Kikeri et al., 1989) but is at variance with results of patch clamp experiments in which it was reported that apical  $\text{K}^+$  channels in inside-out patches of rat TAL did not conduct  $\text{NH}_4^+$  (Bleich et al., 1990). The results of the patch clamp experiments are inconclusive, however, because under the conditions used to test for  $\text{NH}_4^+$  conductance, the channel also did not conduct  $\text{K}^+$  (Bleich et al., 1990). Further studies are needed to assess directly the  $\text{NH}_4^+$  conductive properties of single apical  $\text{K}^+$  channels in the mammalian TAL.

Although barium-sensitive  $\text{NH}_4^+$  uptake occurs in response to luminal  $\text{NH}_4^+$  addition (i.e., in response to the imposition of a large lumen to cell  $\text{NH}_4^+$  concentration difference), several additional observations indicate that this pathway does not contribute significantly to transcellular ammonium absorption under physiologic conditions in which ammonium is present on both sides of the tubule. First, furosemide abolished net ammonium absorption but does not inhibit either the apical  $\text{K}^+$  conductance or the cell negative membrane voltage that would drive diffusive  $\text{NH}_4^+$  entry (Greger et al., 1983; Greger, 1985; Hebert and Andreoli, 1984; Hurst and Hunter, 1992).<sup>4</sup> Second, addition of barium to the tubule lumen reduced

<sup>4</sup> Furosemide causes membrane hyperpolarization, which has been reported to reduce the open probability of apical  $\text{K}^+$  channels; however, this effect is negligible over the range of voltages encountered physiologically (Bleich et al., 1990). Thus, the predominant effect of hyperpolarization should be to increase the driving force for  $\text{NH}_4^+$  electrodiffusion.

net ammonium absorption only by 14% (Table IV). While our data do not exclude the possibility that this reflects direct inhibition of  $\text{NH}_4^+$  uptake (e.g., via apical  $\text{K}^+$  channels), we believe that the small inhibitory effect of  $\text{Ba}^{2+}$  on ammonium absorption is more likely the result of secondary effects of  $\text{Ba}^{2+}$  on two other transport pathways involved in  $\text{NH}_4^+$  absorption: (a) apical  $\text{Na}^+\text{-NH}_4^+(\text{K}^+)\text{-2Cl}^-$  cotransport, which is inhibited by the action of  $\text{Ba}^{2+}$  to depolarize the cell and increase the intracellular  $\text{Cl}^-$  activity (Greger, 1985; Hebert, Reeves, Molony, and Andreoli, 1987), and (b) paracellular  $\text{NH}_4^+$  diffusion, which accounts for a small but significant portion (~20%) of the net ammonium absorptive flux (Good, 1988; Garvin et al., 1988) and is diminished by the effect of  $\text{Ba}^{2+}$  to decrease the transepithelial voltage (Table IV). The slow intracellular alkalization observed following luminal  $\text{Ba}^{2+}$  addition (Fig. 4, Table III) suggests further that this pathway does not mediate rapid uptake of  $\text{NH}_4^+$  and is consistent with a secondary effect of  $\text{Ba}^{2+}$  to diminish apical  $\text{Na}^+\text{-NH}_4^+\text{-2Cl}^-$  uptake. We do not know, however, whether the entire cell alkalization observed with  $\text{Ba}^{2+}$  can be accounted for by a small reduction in apical  $\text{NH}_4^+$  uptake or whether other factors, such as effects of  $\text{Ba}^{2+}$  on cell metabolism or basolateral transport pathways, also may contribute.

Several factors may account for the lack of contribution of the barium-sensitive pathway to apical  $\text{NH}_4^+$  uptake under symmetric ammonium conditions. Rapid uptake of  $\text{NH}_4^+$  on the  $\text{Na}^+\text{-NH}_4^+\text{-2Cl}^-$  cotransporter would have at least two effects that could minimize barium-sensitive  $\text{NH}_4^+$  entry: (a) elevation of the intracellular  $[\text{NH}_4^+]$  to a value above that in the luminal fluid, thereby creating a transmembrane  $\text{NH}_4^+$  concentration difference that opposes  $\text{NH}_4^+$  entry, and (b) acidification of the cells (Tables II and III), which may inhibit  $\text{Ba}^{2+}$ -sensitive  $\text{NH}_4^+$  transport pathways such as the apical  $\text{K}^+$  conductance (Oberleithner et al., 1988; Bleich et al., 1990).

We are grateful to L. Reuss for helpful comments on the manuscript.

This research was supported by National Institutes of Health Grants DK-38217 and DK-01745.

Original version received 2 February 1993 and accepted version received 13 December 1993.

#### REFERENCES

- Bleich, M., E. Schlatter, and R. Greger. 1990. The luminal  $\text{K}^+$  channel of the thick ascending limb of Henle's loop. *Pflügers Archiv*. 415:449-460.
- Chaillet, J. R., and W. F. Boron. 1985. Intracellular calibration of a pH sensitive dye in isolated, perfused salamander proximal tubules. *Journal of General Physiology*. 86:765-794.
- DuBose, T. D., Jr., M. S. Lucci, R. J. Hogg, L. R. Pucacco, J. P. Kokko, and N. W. Carter. 1983. Comparison of acidification parameters in superficial and deep nephrons of the rat. *American Journal of Physiology* 244(Renal Fluid Electrolyte Physiology. 13):F497-F503.
- Garvin, J. L., M. B. Burg, and M. A. Knepper. 1988. Active  $\text{NH}_4^+$  absorption by the thick ascending limb. *American Journal of Physiology*. 255(Renal Fluid Electrolyte Physiology. 24):F57-F65.
- Good, D. W. 1987. Effects of potassium on ammonia transport by medullary thick ascending limb of the rat. *Journal of Clinical Investigation*. 80:1358-1365.
- Good, D. W. 1988. Active absorption of  $\text{NH}_4^+$  by rat medullary thick ascending limb: inhibition by potassium. *American Journal of Physiology*. 255(Renal Fluid Electrolyte Physiology. 24):F78-F87.

- Good, D. W. 1990a. Inhibition of bicarbonate absorption by peptide hormones and cyclic adenosine monophosphate in rat medullary thick ascending limb. *Journal of Clinical Investigation*. 85:1006–1013.
- Good, D. W. 1990b. Adaptation of  $\text{HCO}_3^-$  and  $\text{NH}_4^+$  transport in rat MTAL: effects of chronic metabolic acidosis and  $\text{Na}^+$  intake. *American Journal of Physiology*. 258(Renal Fluid Electrolyte Physiology. 27):F1345–F1353.
- Good, D. W. 1991. Regulation of bicarbonate and ammonium absorption in the thick ascending limb of the rat. *Kidney International*. 40:S36–S42.
- Good, D. W. 1992. Effects of osmolality on bicarbonate absorption by medullary thick ascending limb of the rat. *Journal of Clinical Investigation*. 89:184–190.
- Good, D. W. 1993. The thick ascending limb as a site of renal bicarbonate reabsorption. *Seminars in Nephrology*. 13:225–235.
- Good, D. W., and M. A. Knepper. 1990. Mechanisms of ammonium excretion: role of the renal medulla. *Seminars in Nephrology*. 10:166–173.
- Good, D. W., M. A. Knepper, and M. B. Burg. 1984. Ammonia and bicarbonate transport by thick ascending limb of rat kidney. *American Journal of Physiology*. 247(Renal Fluid Electrolyte Physiology. 16):F35–F44.
- Good, D. W., and G. G. Vurek. 1983. Picomole quantitation of ammonia by flow-through fluorometry. *Analytical Biochemistry*. 130:199–202.
- Greger, R. 1985. Ion transport mechanisms in thick ascending limb of Henle's loop of mammalian nephron. *Physiological Reviews*. 65:760–797.
- Greger, R., and E. Schlatter. 1983. Properties of the lumen membrane of the cortical thick ascending limb of Henle's loop of rabbit kidney. *Pflügers Archiv*. 396:315–324.
- Greger, R., E. Schlatter, and F. Lang. 1983. Evidence for electroneutral sodium chloride cotransport in the cortical thick ascending limb of Henle's loop of rabbit kidney. *Pflügers Archiv*. 396:308–314.
- Guggino, W. B., H. Oberleithner, and G. Giebisch. 1988. The amphibian diluting segment. *American Journal of Physiology*. 254(Renal Fluid Electrolyte Physiology. 23):F615–627.
- Hebert, S. C. 1986a. Hypertonic cell volume regulation in mouse thick limbs I. ADH dependency and nephron heterogeneity. *American Journal of Physiology*. 250(Cell Physiology):C907–C919.
- Hebert, S. 1986b. Hypertonic cell volume regulation in mouse thick limbs II.  $\text{Na}^+$ - $\text{H}^+$  and  $\text{Cl}^-$ - $\text{HCO}_3^-$  exchange in basolateral membranes. *American Journal of Physiology*. 250(Cell Physiology. 19):C920–C931.
- Hebert, S. C., and T. E. Andreoli. 1984. Effects of antidiuretic hormone on cellular conductive pathways in mouse medullary thick ascending limbs of Henle: II. Determinants of the ADH-mediated increases in transepithelial voltage and in net  $\text{Cl}^-$  absorption. *Journal of Membrane Biology*. 80:221–233.
- Hebert, S. C., and T. E. Andreoli. 1986. Ionic conductance pathways in the mouse medullary thick ascending limb of Henle. *Journal of General Physiology*. 87:567–590.
- Hebert, S. C., W. B. Reeves, D. A. Molony, and T. E. Andreoli. 1987. The medullary thick ascending limb: function and modulation of the single-effect multiplier. *Kidney International*. 31:580–588.
- Hurst, A. M., and M. Hunter. 1992. Apical membrane potassium channels in frog diluting segment: stimulation by furosemide. *American Journal of Physiology*. 262(Renal Fluid Electrolyte Physiology. 31):F606–614.
- Kikeri, D., A. Sun, M. L. Zeidel, and S. C. Hebert. 1989. Cell membranes impermeable to  $\text{NH}_3$ . *Nature*. 339:478–480.
- Kikeri, D., A. Sun, M. L. Zeidel, and S. C. Hebert. 1992. Cellular  $\text{NH}_4^+/\text{K}^+$  transport pathways in mouse medullary thick limb of Henle. *Journal of General Physiology*. 99:435–461.

- Kinne, R., E. Kinne-Saffran, H. Schutz, and B. Scholermann. 1986. Ammonium transport in medullary thick ascending limb of rabbit kidney: involvement of the  $\text{Na}^+$ ,  $\text{K}^+$ ,  $\text{Cl}^-$ -cotransporter. *Journal of Membrane Biology*. 94:279–284.
- Knepper, M. A., R. Packer, and D. W. Good. 1989. Ammonium transport in the kidney. *Physiological Reviews*. 69:179–249.
- Kone, B. C., K. M. Madsen, and C. C. Tisher. 1984. Ultrastructure of the thick ascending limb of Henle in the rat kidney. *American Journal of Anatomy*. 17:217–226.
- Krapf, R. 1988. Basolateral membrane  $\text{H}^+/\text{OH}^-/\text{HCO}_3^-$  transport in the rat cortical thick ascending limb. Evidence for an electrogenic  $\text{Na}^+/\text{HCO}_3^-$  cotransporter in parallel with a  $\text{Na}^+/\text{H}^+$  antiporter. *Journal of Clinical Investigation*. 82:234–241.
- Oberleithner, H., U. Kersting, and M. Hunter. 1988. Cytoplasmic pH determines  $\text{K}^+$  conductance in fused renal epithelial cells. *Proceedings of the National Academy of Sciences*. 85:8345–8349.
- Rink, T. J., R. Y. Tsien, and T. Pozzan. 1982. Cytoplasmic pH and free  $\text{Mg}^{2+}$  in lymphocytes. *Journal of Cell Biology*. 95:189–196.
- Roos, A., and W. Boron. 1981. Intracellular pH. *Physiological Reviews*. 61:296–434.
- Thomas, J. A., R. N. Buchsbaum, A. Zimniak, and E. Racker. 1979. Intracellular pH measurements in Ehrlich ascites tumor cells utilizing spectroscopic probes generated in situ. *Biochemistry*. 18:2210–2218.
- Watts, B. A., III, and D. W. Good. 1990. Effects of  $\text{NH}_4^+$  transport on intracellular pH in rat medullary thick ascending limb. *Journal of the American Society of Nephrology*. 1:660. (Abstr.)
- Wingo, C. S. 1986. Effect of acidosis on chloride transport in the cortical thick ascending limb of Henle perfused in vitro. *Journal of Clinical Investigation*. 78:1324–1330.